The Equivalent Thermal Resistance of Tile Roofs with and without Batten Systems

Rick Olson

William Miller, PhD
Member ASHRAE

Russell Graves

ABSTRACT

A clay roof, several concrete tile roofs, and one conventional direct-nailed shingle roof were installed on a fully instrumented attic test facility operating in east Tennessee's climate. The roof tiles were attached to batten and counter-batten systems and also fastened directly to the deck to observe the benefits of the venting occurring between the roof's sheathing and the profiled tile. Roof, attic, and deck temperatures and heat flows were recorded for each of the tile roofs and for the attic cavity covered with a conventionally pigmented and direct-nailed asphalt shingle roof. The data were used to benchmark a computer tool for simulation of roofs and attics and the tool used to develop an approach for computing an equivalent seasonal R-value for sub-tile venting. The approach computed the heat flux through the ceiling of the direct-nailed shingle roof and also the flux crossing the ceiling of a ventilated tile roof. The load for the shingle roof and attic was made equivalent to the load crossing the ceiling of the tile roof and attic by modifying the amount of ceiling insulation for the shingle assembly until both attics had the same annual load. The added R-value equates to the effective annual thermal resistance for the tile roof having different combinations of surface radiation properties (cool color pigments) and or building constructions. Therefore the direct nailed shingle roof served as a control for estimating the equivalent thermal resistance of the air space. Simulations were benchmarked to data in the ASHRAE Handbook—Fundamentals *for the thermal resistance of inclined and closed air spaces.*

INTRODUCTION

The venting of the underside of roof tile provides thermal benefits for comfort cooling. Residential roof tests by Beal and Chandra (1995) demonstrated a 45% reduction in the daytime heat flux penetrating a counter-batten tile roof as compared to a direct nailed shingle roof. Parker et al. (2002) measured an 8% reduction in annual cooling load for a home with terra cotta barrel-shaped tile as compared to an adjacent, identical footprint home with asphalt shingle roof. These reported energy savings are in part attributed to the venting that occurs on the underside of the roof tile, although it is difficult to quantify this benefit.

The reduced heat flow occurs because of a thermally driven airflow within the air gap formed between the tile and the roof deck. The thickness of the air space depends on the construction practice whether laid direct-to-deck, fastened to battens or attached to double-battens. For double-batten construction, wood furring strips are laid vertically (soffit-to-ridge) against the roof deck and a second batten running parallel to the roof's ridge is laid horizontally across the vertical counter-battens (Figure 1). The bottom surface of the inclined channel is formed by the sheathing (oriented strand board [OSB] deck) and 30# felt paper placed on top of the sheathing. The underside of the roof tiles establish the upper surface of the inclined channel, and the tile overlaps are designed to be air porous to allow pressure equalization and reduce the wind uplift on the tiles. The airflow in the inclined channel is driven more by buoyancy than by wind-driven forces because building codes require fire stops be used to block any path for potential burning embers to enter the inclined channel. The air gap also provides an improvement in the insulating effect of the roof system. However, measuring and correctly describing the

Rick Olson *is the technical director for the Tile Roof Institute, Eugene, Oregon.* ***William Miller*** *serves as a building scientist at the Oak Ridge National Laboratory, Oak Ridge, TN.* ***Russell Graves*** *is an undergraduate student studying Mechanical Engineering at the University of Tennessee, Knoxville, TN.*

Published by ASHRAE 2013

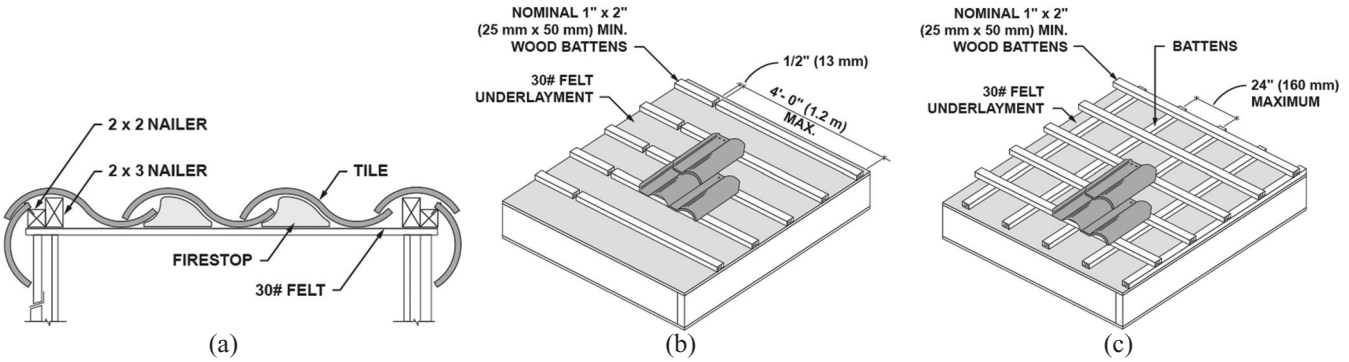

Figure 1 *The attachment of tile (a) direct-to-deck, (b) mounted on battens, and (c) mounted on double-battens.*

heat flow within the cavity of a tile roof is a key hurdle for predicting the roof's thermal performance.

IECC (2012) and ASHRAE 90.2 (2007) do not directly address sub-tile ventilation. Title 24 of the California Energy Commission (CEC 2008, Section 152) specifies that steep-slope roof products with a density of 5 pounds per square foot or more shall have a minimum aged solar reflectance of 0.15 and a minimum thermal emittance of 0.75 in all California climates. The CEC allows several exceptions for the solar reflectance and emittance requirements, and two of the exceptions are pertinent to work described herein:

1. Exception granted if insulation with a thermal resistance of at least 0.85 (h·ft^2·°F)/Btu [0.15 (m^2·°C)/W] or at least a ¾ in. (0.02 m) air space is added to the roof deck; or
2. R_{US}–3 (R_{SI}–0.53) or greater roof deck insulation is placed above the vented attic (exception applicable for climate zones 10, 11, 13 and 14).

A combined experimental and analytical study therefore documented the effective annual thermal resistance of the inclined and opened air space formed by clay and concrete tile applied direct-to-deck, applied on battens, and applied on double batten systems. The batten and double batten assembly were studied to determine added benefit for elevating tile off the roof deck and to also assess systems that would provide a free flow path between the tile and the roof deck (see Pennington comment on blockage in air space made at CEC workshop [Peters, 2006]). Tile roofs were selected having high-, medium-, and flat-profiles.

TILE ROOF AND ATTIC TEST STAND

The experimental portion of the study included testing of attic assemblies on the Envelope Systems Research Apparatus (ESRA). All attics were equipped with heat flux transducers (HFTs) embedded in the roof deck and in the attic floor. A Fox 670 heat flux apparatus was used to calibrate each HFT in a guard made of the same material used in construction to correct for shunting effects (i.e., distortion due to three-dimensional heat flow, ASTM [2006]). Salient features of the ESRA and instrumentation details of the roof and attic assemblies are provided by Miller (2006). A commercially available asphalt shingle with a solar reflectance of 0.093 and thermal emittance of 0.89 (SR10E89) served as the control for comparing the thermal performances of the prototype roof systems. Solar reflectance (SR) was measured using the ASTM protocol C 1549 (2009). Thermal emittance (TE) was measured using the ASTM protocol C 1371 (2004).

The field data were used to benchmark the attic simulation code AtticSim (ASTM C 1340 2004). Ceiling insulation in the test assemblies was purposely set low at R_{US}–5 (h·ft^2·°F)/Btu (R_{SI}–0.9 [m^2·K]/W) to help reduce the experimental uncertainty in measured heat flux. Hence, the discussions of field data will focus on heat crossing the roof deck of the attic, and simulations will provide results for energy consumption of attics with code-compliant levels of insulation.

CONCRETE TILE FIELD DATA

Miller and Kosny (2008) assessed the effects of cool color roofs, thermal mass, and placement of batten and double-batten systems under tile roofs. Miller and Kosny observed that medium-profile tiles exhibited less heat transfer across the roof deck as compared to a conventional shingle roof. Most important, though, is the results among the medium-profile tile; the one with conventional color pigments (0.10 solar reflectance) and on double battens (1.5 in [0.038 m]) had measured deck heat transfer very similar to that of the cool color tile (0.40 solar reflectance) attached directly to the deck. Therefore, for the two tiles, the nominal 1.5 in (0.038 m) inclined air space is as effective as is the benefit derived from cool color roofs. The performance of the air space agrees with similar work by Beal and Chandra (1995), who field-tested two identical medium-profile concrete tile roofs; one tile roof was direct-nailed and the other was offset mounted about 1½ in. (0.038 m) above the deck. Beal and Chandra (1995) measured an 11% reduction in the daytime heat flux penetrating the concrete tile roof on double battens compared with the adjacent direct-nailed tile roof.

Miller et al. (2005) field tested flat concrete tile (SR13E83) and a medium-profile tile (SR10E93) that had very similar solar reflectance and thermal emittance to the control, an asphalt shingle (SR10E89) roof (Figure 2). The heat transfer through the roof and ceiling of the attic with the flat concrete roof and the medium-profile tile roof were about half that measured for the asphalt shingle roof (Figure 2). The reduction is due to the buoyancy effects occurring in the inclined air channel that dissipates heat away from the deck. The flat concrete tiles are attached to batten and counter-batten strips, which form a vent cavity that is about 1½ in. (0.038 m) deep. The medium-profile tile is on battens and also forms its own half-cylindrical channel of about 0.5 in. (0.0127 m) radius.

Bulk air and sheathing temperatures for the flat concrete tile (heat flux depicted in Figure 2) were measured along the length of the tile roof from soffit to ridge (Figure 3). Data is displayed for a hot August day and also for a cold day in January to view the differences between hot and cold weather.

August (8/17/2004) field data: At 8 AM the air in the inclined cavity and the sheathing temperatures are about the same from the soffit to the ridge vent. As the day progresses,

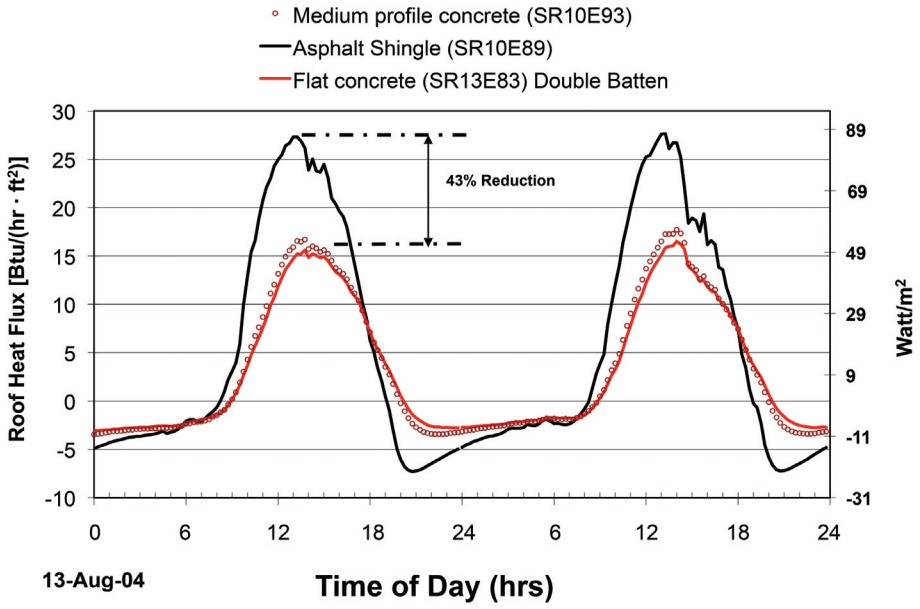

Figure 2 *Heat penetrating the roof of each attic assembly being field tested on the ESRA (Miller et al. 2005).*

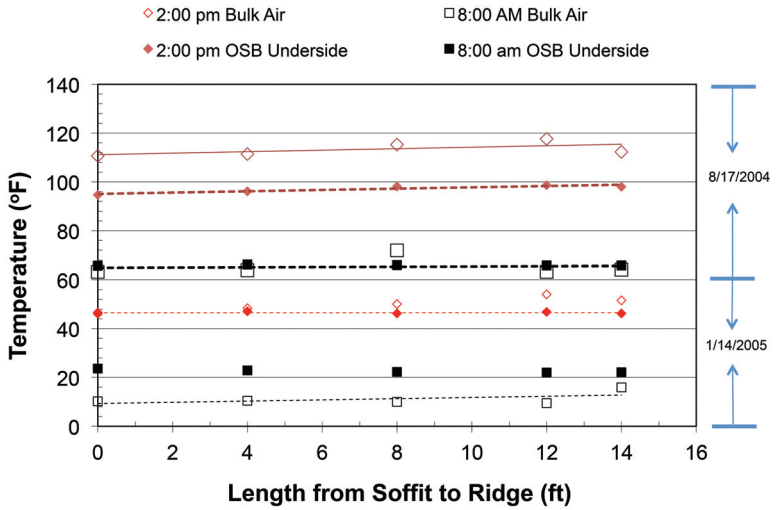

Figure 3 *Local temperature measures for a flat concrete tile made along the length of the inclined air space at 8:00 a.m. and at solar noon (2:00 p.m.).*

irradiance heats the roof and there is observed a linear increase in the sheathing's underside temperature; it being about 94.5°F (34.7°C) near the soffit and increasing to 98°F (36.6°C) just upstream the ridge vent. The linear profile is expected because the irradiance has no preferred location on the south-facing roof deck, implying a constant solar flux. The bulk air temperature in the inclined air space is observed to be roughly 20°F (10.5°C) warmer than the sheathing (Figure 3). Its profile dips as the air nears the ridge vent. The tiles are designed porous to alleviate wind uplift and therefore opposing winds at or around the ridge are possibly causing the slight drop. The bulk air temperature is about 30°F (16.7°C) warmer than the outdoor air.

January (1/14/2005) field data: At 8 a.m. the bulk air temperature measured near the soffit is 13°F (7.2°C) less than the sheathing's underside temperature (Figure 3). This temperature difference lessens as one moves from the measurement station at the soffit to the station at the ridge. Night sky radiation causes the tile roof to chill below the outdoor air temperature, and therefore air in the inclined air space is cooled below the outdoor air temperature and is believed to flow from ridge to soffit as the tile cools the air in the channel. At solar noon there is only a slight increase in the bulk air temperature occurring around 12 feet (3.6 m) from the soffit. However, the irradiance has caused a flow reversal in the channel whereby flow is not from soffit to ridge simply because of the air temperatures as affected by the tile roof.

ALGORITHM FOR SUB-TILE VENTILATION

Miller et al. (2007) previously benchmarked AtticSim against the field data for stone-coated metal roofs fixed to double-battens. The tool has also been validated in this study against the tile field experiments (Figures 2 and 3) and predicted the ceiling heat flow within ±10% of the field measure. The tool contains overall moisture balances but is not designed to predict moisture content of wood surfaces.

The airflow in the inclined air space can be driven by both buoyancy and wind; however, the air space is obstructed at the soffit to resist burning embers landing on the structure and to resist flame impingement (Quarles and TenWolde 2004). Therefore, the flow phenomenon is driven more by natural convection rather than by forced convection because the fire code calls for an obstruction which for tile roofs takes the form of fire stops[1] which still allows for outdoor makeup air. Blocking the eave also helps alleviate wind uplift on the offset-mounted roof. Hence, by fire code and wind design, the formulation of the algorithm is based solely on natural convection flow fields within the air space of the offset mounted roof system.

Hollands et al. (1976); Arnold, et al. (1974); Azevedo and Sparrow (1985), and, most recently, Brinkworth (2000) studied the air flows occurring in inclined air channels. During winter exposure, the warmer roof deck is positioned below the cooler roof cover and heat flows upwards through the roof, much as in the problem studied by Hollands et al. (1976) for a closed cavity. Here, a denser air layer near the roof's underside overlies lighter air adjacent to the roof deck. The density inversion causes the heat transfer across the air channel to switch from conduction to single-cell convection to Bénard cell convection, depending on the magnitude of the Ra_S number. For Ra_S numbers of less than 1708/cos(θ), there is no naturally induced airflow within the cavity, and the heat transfer occurs exclusively by conduction. However, as the flow increases as a result of buoyancy, the heat transfer within the channel can switch to Bénard cell convection.

During summer exposure, the roof cover is hotter than the roof deck, and Bénard cell convection does not occur within a closed inclined air space because the lighter air layer is naturally above the denser air layer. Arnold et al. (1974) offers a correlation which is based on an adaptation of heat transfer in a vertical closed cavity; it being

$$\mathrm{Nu}(\theta) = 1 + [\mathrm{Nu}_{90^\circ} - 1]\sin(\theta) \qquad (1)$$

where Nu_{90° is estimated from the correlations by ElSherbiny et al. 1984, and θ is the angle of inclination the roof makes with the horizontal plane.

The correlation by Azevedo and Sparrow (1985) is used for the case of an open inclined air space. Their correlation was developed from experimental data where both walls were heated, the top wall heated with the bottom wall unheated, and also for the case of the top wall unheated and the bottom wall heated. Several inclinations and channel heights were studied and used to derive the following correlation which is programmed in an algorithm for open channels:

$$\mathrm{Nu} = 0.673\left[\frac{S}{H}\mathrm{Ra}_S\right]^{0.25}$$

where

S = the height of the air space

H = the length of the roof from soffit to ridge

Ra_S = the Rayleigh number for an inclined air space of S height.

The algorithm in AtticSim was benchmarked against the *ASHRAE Handbook—Fundamentals* (1989) data for closed inclined air spaces, Table 1. Two effective emittance values were investigated to review the computed R-value. If the thermal emittance of the two facing surfaces are high at 0.90 then radiation heat transfer dominates over convention in the closed cell. However, if one of the two surfaces has a low emittance (i.e., 0.05 to 0.25) then convection heat transfer dominates.

The computed R-value by AtticSim for a closed air space is within 1.5% of ASHRAE measures (Table 1) if there are no low-emittance surfaces. The inclusion of a low-e surface showed an error of 6.7% for a 0.75 in. (0.019 m) air space and an error of 12% for the larger air space of 1.5 in (0.038 m). The

1. Tile industry uses the term *bird stop* for keeping rodents and birds from entering and nesting in the inclined air space.

mean air temperature in the air space and the temperature change (ΔT) across the air space were gleaned from summer field data collected at solar noon. AtticSim and ASHRAE (Yarbrough and Desjarlais 1991) algorithms fixed these temperatures and computed the thermal resistance of the air space. Note that changing the air temperature and the temperature drop across the air space changes the value of the thermal resistance.

If one of the surfaces has low-emittance, then the thermal resistance is seen to increase by almost a factor of 5 over the case of the closed channel with high emittance surfaces, Table 1.

The results imply that inclusion of a reflective underlayment or painting the underside of the tile with low-emittance paint will enhance performance of tile roofs. Therefore simulations were conducted with and without a low emittance surface in the air space.

Climatic Simulation Results

The AtticSim code was used in conjunction with Energy Plus to compute the equivalent annual thermal resistance of the inclined air space under tile roofs. The standardized HERS BESTEST home (NREL 1995) clad with clay and concrete tile roofs was simulated for several cities each in a unique ASHRAE climate zone, Table 2. Sacramento, CA was included but with ceiling insulation set to Title 24 building code. Energy Plus estimated the hourly run times for the HERS BESTEST home (NREL 1995) conditioned by an air-conditioner certified with a Seasonal Energy Efficiency Ratio (SEER) of 13 and heated by an 85%. efficient gas furnace.

Table 1. Benchmark of the Effective Thermal Resistance Computed by the AtticSim Code as Compared to *ASHRAE Handbook—Fundamentals* (1989) Data

	ε_{eff}	Air Space ΔT, °F (°C)	Mean Air Temperature, °F (°C)	Thermal Resistance[2] (°F · ft^2 ·h)/Btu ASHRAE[1]	AtticSim	% Error
0.75 in. (0.019 m)	0.7456	13.7 (7.61)	130.4 (54.7)	0.762	0.752	1.22%
Air space	0.0497	33.3 (18.5)	123.3 (50.7)	2.976	2.775	6.76%
1.5 in. (0.038 m)	0.7456	14.7 (8.17)	130.0 (54.4)	0.814	0.818	0.49%
Air space	0.0497	37.7 (20.9)	121.8 (49.9)	3.191	3.588	12.44%

1 Yarbrough and Desjarlais (1991) and ASHRAE Handbook—Fundamentals, (1989) Chapter 22.2, Table 2.
2 R_{SI} [(m^2 ·K)/W] = R_{US}/5.678

Table 2. Simulations Conducted in the ASHRAE Climate Zones to Estimate the Benefit of Sub-Tile Ventilation. IECC 2009 Code Assumed for Ceiling R-value

ASHRAE Zone	City	State	HDD_{65}	CDD_{65}	Ceiling R-value [h · ft^2 · °F)/Btu]
1	Miami	FL	222	9368	30
2	Austin	TX	1481	7435	30
3	Atlanta	GA	2614	4814	30
4	Baltimore	MD	4731	3598	38
5	Chicago	IL	6139	2895	43
6	Minneapolis	MN	7787	2513	49
7	Fargo	ND	10052	1332	49
8	Fairbanks	AK	13940	1040	52
Title 24	Sacramento	CA	2697	1202	38

AtticSim used these outputs from Energy Plus to better estimate the roof and attic load as coupled to the building envelope. The attic floor was modeled assuming no air leakage crossing the attic floor. Ducts for the air conditioner were assumed in the conditioned space.

The TRI and its affiliates provided specifications for several tiles with high-, medium-, and flat profile, see Appendix A. Members computed the volume of the air space made by tiles applied direct-to-deck and derived an effective height of the tile's air space by dividing the underside volume by the footprint for a square (100 square feet [9.3 m^2]) of tile. Elevations adjustments were made for batten and double-batten systems, but the volume of wood within the footprint was subtracted from the total volume in determining the effective height of the air space. Simulations used the effective air space and results for all tile with the tile attached directly to the deck, the tile placed on battens, and the tile fastened to double batten assemblies is provided in Appendix B.

A procedure was formulated that matched the annual load crossing the ceiling of a tile roof and attic as compared to the load computed for a direct-nailed shingle roof (Figure 4). As example, an asphalt shingle roof with solar reflectance of 0.10 and thermal emittance of 0.90 was simulated for the climate of Miami, Florida; annual load crossing the ceiling was 4.25 MBtu/yr (4483 MJ/yr) assuming R_{US}–30 (R_{SI} 5.3) of insulation on the attic floor. The same home but with a tile roof placed on double battens needed R_{US}–25.3 (R_{SI} 4.5) to match the load of the home with a shingle roof.

Therefore, the equivalent annual R-value of the inclined air space is estimated at R_{US}–4.7 = [R_{US}–30 – R_{US}–25.3]. The computed R-value is termed an equivalent annual value because it accounts for the diurnal and seasonal changes in mean air temperature and temperature change across the inclined air space, which in turn affects the temperatures and heat flows within the attic. Results imply what the added level of ceiling insulation needs to be for the control shingle roof to have the same annual load as the tile roof.

The field data for summer shown back in Figure 3 reveals that the open air space helps drop the heat flow crossing the roof deck which, in turn, drops the underside temperature of the deck and the radiation and convection heat transfer crossing from the deck to the attic floor. As the surface temperatures of the roof and attic vary so does the radiation and convection heat transfer coefficients; however, by comparing the ceiling load for the attic with tile roof to the base shingle roof, the effect of the air space on attic temperatures and subsequently the heat flows is accounted for in prediction of the equivalent annual thermal resistance. Therefore the procedure does not yield a true academic measure of thermal resistance for the air space, rather we computed an effective annual resistance needed to match load to the base shingle roof assembly.

Direct-to-Deck ε_{eff} = 0.82 Simulation Results

AtticSim/Energy Plus simulations for the concrete and clay tile fastened directly to the deck show best results in the hottest US climates (Figure 5). The tiles with high profile (Espana and Barcelona 900) yielded the highest thermal resistance of all tile. In Miami, Florida (ASHRAE zone 1) these tiles yielded an annual equivalent R_{US}–2.7, which implies that for a conventional shingle roof to have the same annual ceiling

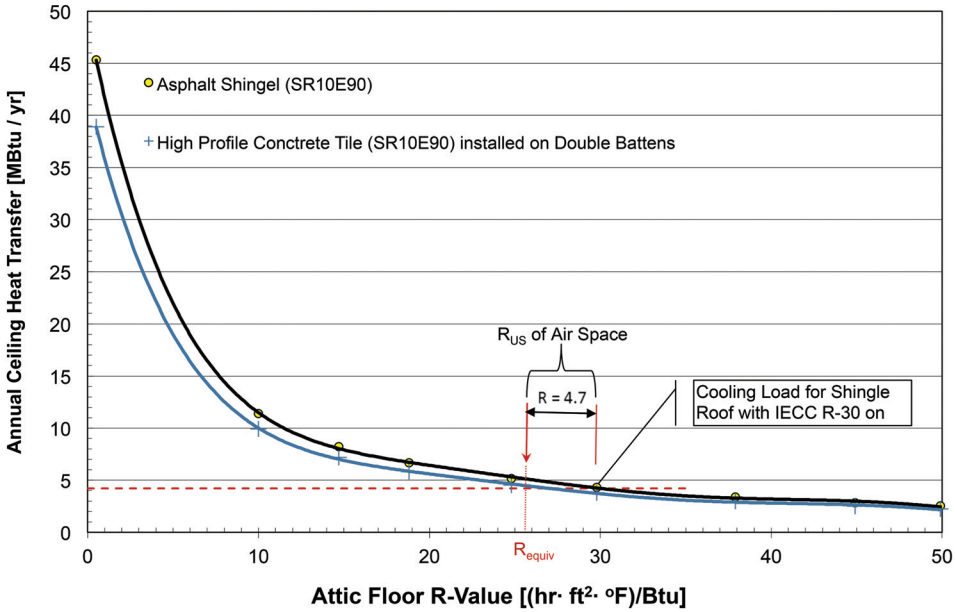

Figure 4 *Annual load crossing the ceiling of home simulated for Miami, Florida with shingle roof and with concrete tile roof placed on double battens. The R-value of ceiling insulation needed to match load for shingle roof is used to estimate the equivalent R-value of the inclined air space.*

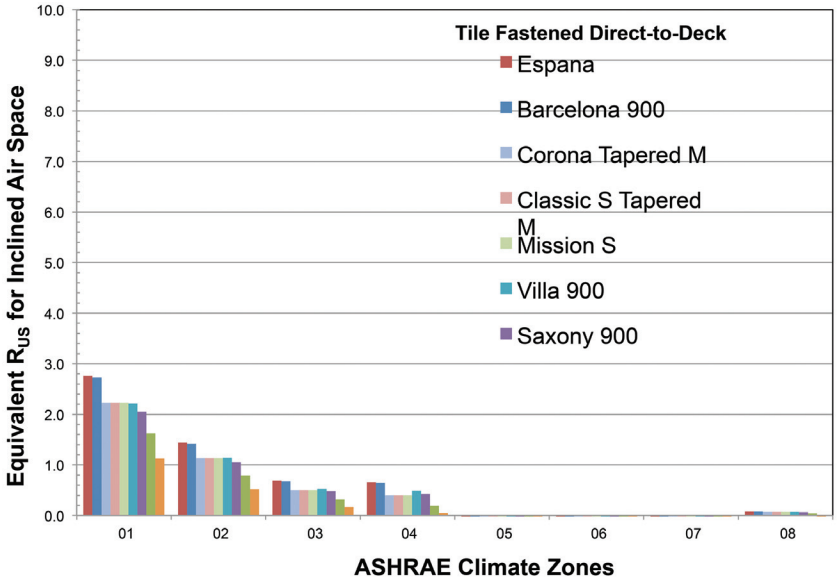

Figure 5 *The annual equivalent thermal resistance for DtD tile roofs;* $\varepsilon_{eff} = 0.82$.

load, it would need R_{US}–2.7 more insulation above ASHRAE 90.2 (2007) code requirement. Or said differently, the inclined air space formed by the Barcelona 900 and Espana tile with code level of insulation on the attic floor represents an equivalent annual R_{US} of 2.7 [(h·ft^2·°F)/Btu]; R_{SI} of ([0.48 m^2·°C]/W).

The high profile clay tiles, Corona Tapered M, Classic S Tapered M, and Mission S) all yielded an equivalent thermal resistance of about R_{US}–2.2 (R_{SI}–0.39) for exposure in Miami, Florida. In Austin, Texas (Zone 2) the equivalent thermal resistance drops to about R_{US}–1.1 (R_{SI}–0.19). The medium profile tiles (Villa 900) show results very similar to the clay tile roofs. The Saxony 900, Madera, and Eagle FT tile, because of their flat profile, had the lowest computed equivalent thermal resistance measures (Figure 5).

In climate zone 3 (Atlanta, Georgia), the R-value is of the order 0.7 to 0.2, and in the moderate climate of Baltimore, Maryland (zone 4) the equivalent annual R-value is about 0.2. The more predominantly heating climates of Chicago, Minneapolis, Fargo, and Fairbanks showed that the inclusion of the air space had no impact on thermal performance (Figure 5).

Direct-to-deck ε_{eff} = 0.22 Simulation Results

Additional AtticSim/Energy Plus simulations were made for the case of the tile's underside spray painted with a low-emittance paint having a thermal emittance of 0.22. The concrete and clay tile were again fastened directly to the deck (Figure 6). The low emittance paint increased the effective annual thermal resistance of all tile assemblies (Figure 6). Comparing Figure 5 to 6 reveals that the low emittance paint reduces the radiation heat transfer crossing the air space and therefore improves the thermal resistance. Even the cold climates show some resistance value for the air space; of the order R_{US}–0.5 (R_{SI}–0.09).

For ASHRAE zone 3 (Atlanta, Georgia) the high-profile concrete and clay tiles (Espana, Barcelona 900, Corona Tapered, Classic S, and Mission S) all showed an almost tripling of the effective annual thermal resistance with the addition of the low emittance paint. The clay tiles all jumped from R_{US}–0.5 (R_{SI}–0.09) to R_{US}–1.6 (R_{SI}–0.28).

Double Batten Simulation Results

AtticSim/Energy Plus simulations for Austin, Baltimore and Minneapolis were made with the tile offset mounted on battens and double battens. Figure 7 provides results for double batten applications with the air space having an effective thermal emittance of 0.05, 0.21, and 0.82, respectively. Appendix B lists results for flat-, medium-, and high-profile tile attached direct-to-deck, and on batten and double batten applications.

An underlayment is typically designed to provide hygrothermal protection for the roof deck. Some also offer a low-emittance foil. The foil's emittance is about 0.05 and if used in the air space would further reduce the radiation heat transfer crossing the air space. Because it is positioned facing up, the low-emittance surface is expected to degrade as fine dusts settle and tarnish the foil. Dust accumulation over time was shown to reduce the effectiveness of foil placed on an attic floor (Fairey, Swami, and Beal 1988). However, simulations were made to document feasible gains in performance. More work is needed to document the sustained effectiveness of the foil when used as an underlayment for tile roof applications.

In the hot climate of Austin, the effective annual thermal resistance of the Barcelona and Espana concrete tile applied on double battens increases from R_{US} 1.54 (R_{SI}–0.27)

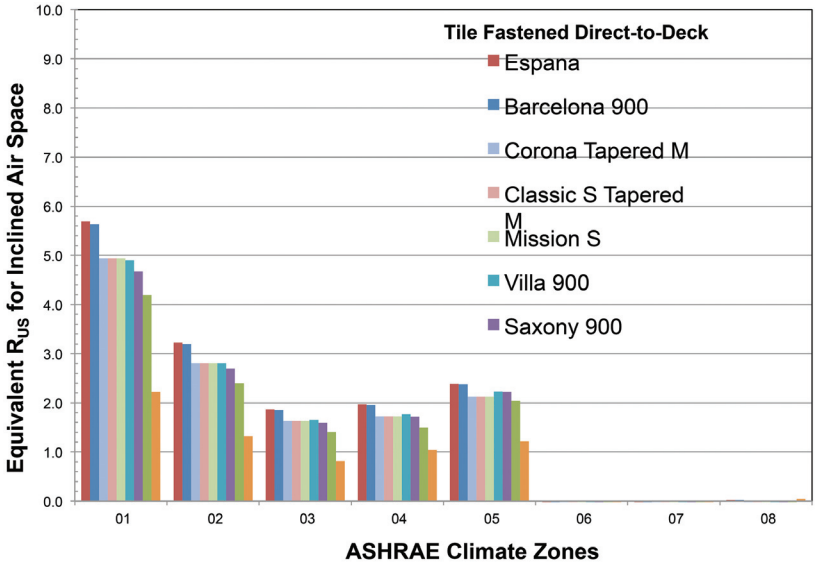

Figure 6 *The annual equivalent thermal resistance for direct-to-deck tile roofs;* $\varepsilon_{eff} = 0.21$.

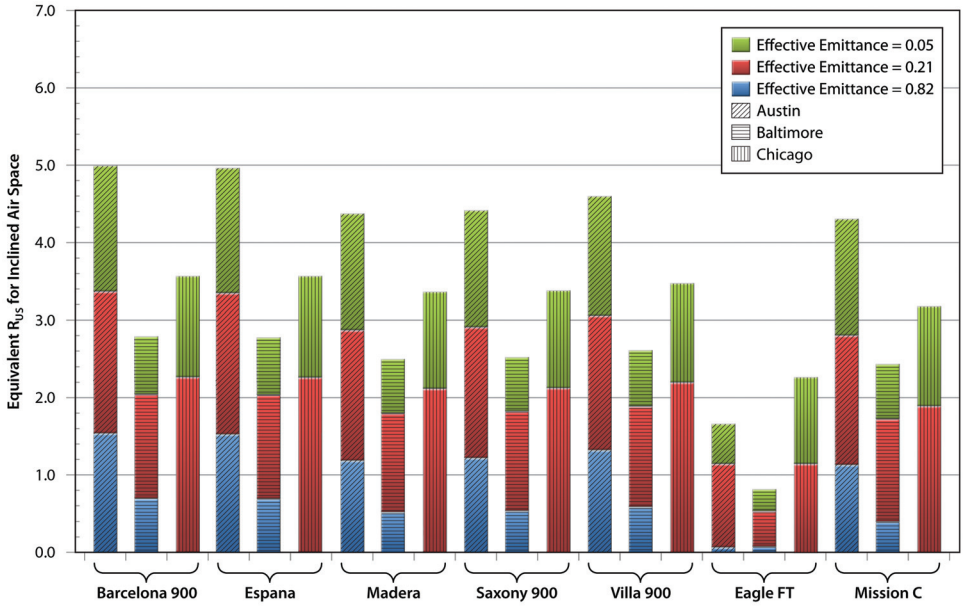

Figure 7 *Simulations for Atlanta, Georgia showing the annual equivalent thermal resistance for tile roofs offset mounted on double battens fastened to the deck.*

(air space $\varepsilon_{eff} = 0.82$) to R_{US} 3.4 (R_{SI}–0.60) (air space $\varepsilon_{eff} = 0.21$) up to a thermal resistance of R_{US}–5 (R_{SI}–0.88) if air space $\varepsilon_{eff} = 0.05$. The Mission C clay tile by practice is fastened direct-to-deck but is also shown in Figure 8 to view its performance against the concrete tiles on double battens. The Mission C yields an effective thermal resistance of R_{US}–4.3 (R_{SI}–0.76) which is just 14% less than that of the best performing concrete tile on double battens. Baltimore is more moderate in climate and maximum effective annual thermal resistance was about R_{US}–1.5 (R_{SI}–0.26) for the case having an $\varepsilon_{eff} = 0.05$. In Minneapolis, the effective annual thermal resistance is only R_{US}–0.60 (R_{SI}–0.1).

Miller (2011) developed design guidelines for roofs and attics and showed that the inclusion of the foil in an inclined air space would yield annual savings of about $80 for simulation in Austin but in the colder climates of Baltimore and Minneapolis savings is only about $10 annually. However, closer inspection shows that the inclusion of a foil in the inclined air space would increase the temperature on the underside of the roof deck during the cold evening hours as

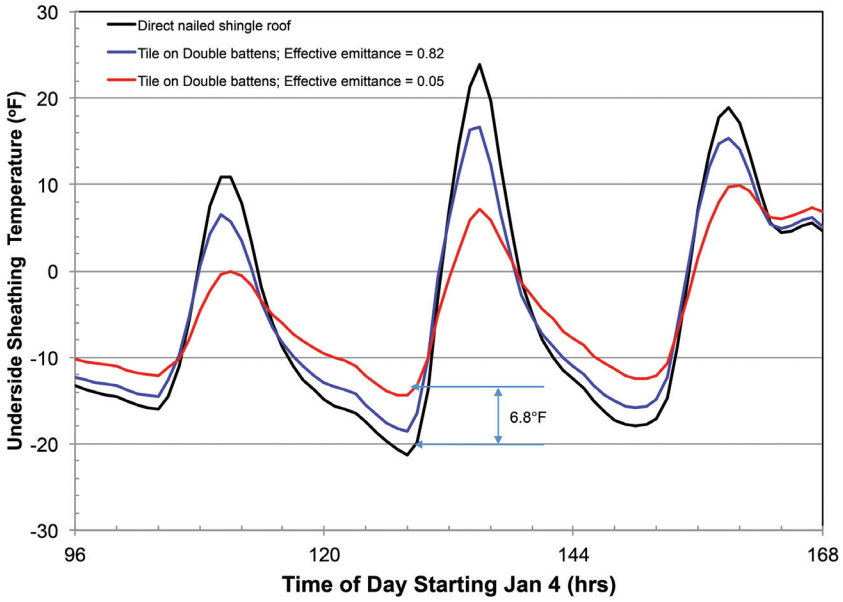

Figure 8 *Simulations for Minneapolis, Minnesota, showing the temperature of the OSB deck facing into the attic for tile roofs on double battens with and without a low emittance surface and also for a direct nailed shingle roof. Data depicted for winter exposure from January 4 through 6.*

compared to a direct nailed shingle roof (Figure 8). All roofs have about the same exterior roof temperature after a cold winter evening. However, at about 8 a.m. the tile roof with low-e foil shows its deck temperature (facing into the attic) to be 7°F (3.9°C) warmer than that computed for the direct nailed shingle roof.

The foil retards the radiation loss to the night sky and keeps the attic and subsequent surfaces warmer than the direct nailed base case. The warmer deck implies that the ventilated attic with tile on double battens has less potential for condensate to form on the underside of the deck as compared to the conventional ventilated and direct nailed roof and attic.

CONCLUSIONS

An inclined air space in or above the roof deck provides thermal buffering and is an excellent design strategy for reducing roof heat gains and losses in hot climates. Field tests of flat concrete tile and medium-profile concrete tile having almost the same solar reflectance and thermal emittance as a conventional shingle roof demonstrated peak day heat flows penetrating the roof deck that were 43% less than that measured for the control shingle roof. Hygrothermal performance also improves because the natural ventilation occurring in the air space during the day helps dry the roof. Thermal resistance of the air space increases if the effective thermal emittance of the air space is reduced by adding a foil (low-emittance surface) or low-emittance paint. Dropping the effective emittance drops the radiation heat transfer crossing the air space and at night causes the temperature of the sheathing's underside to not drop as much as compared to the case without the foil. Therefore, natural ventilation helps dry the roof during the day and the foil surface drops the potential for condensation on the underside of the sheathing during the winter's coldest evening hours.

Field temperatures collected within the air space from soffit to ridge show the heat transfer to be constant flux at the roof deck. At solar noon the bulk air temperature is about 30°F (16.7°C) warmer than the outdoor air and the natural convection flow is transitioning from laminar to turbulent flow as flow proceeds toward the ridge.

A procedure was formulated and validated for predicting the effective annual thermal resistance of the air space. First, an algorithm for combined convection and radiation in a closed air space was benchmarked against published data (*ASHRAE Handbook—Fundamentals* 1989). Second a computer tool, AtticSim with support from Energy Plus, modeled the HERS BESTTEST standard simulation and applied the code to several climates across the U.S. Finally, results were compared to a control shingle roof having the same solar reflectance and thermal emittance as the concrete and clay tile roofs. Fixing the annual load for the control shingle with code level of insulation on the ceiling and comparing the ceiling thermal resistance needed to yield the same load for a tile roof yields the annual effective thermal resistance of the inclined air space.

Tiles with a high profile yielded the highest thermal resistance of all tile. Offset mounting of all tiles improves the thermal resistance; however, best results were observed only in hot to mild climates. The more predominantly cold climates showed no thermal advantage for inclusion of the air space.

However, adding a low emittance surface to the air space causes a significant jump in the effective annual thermal resistance. In the hot climate of Austin, the effective annual thermal resistance of the high profile tile applied on double battens increases from R_{US} 1.54 (R_{SI}–0.27) (air space $\varepsilon_{eff} = 0.82$) to R_{US} 3.4 (R_{SI}–0.60) (air space $\varepsilon_{eff} = 0.21$) up to a thermal resistance of R_{US}–5 (RSI–0.88) if (air space $\varepsilon_{eff} = 0.05$).

ACKNOWLEDGMENTS

Funding for this project was provided by the Tile Roofing Institute under a DOE User Agreement, UR-07-580 and by the Department of Energy Building Technology program. Oak Ridge National Laboratory is managed by UT-Battelle, LLC, for the US Department of Energy under contract DE-AC05-00OR22725. The submitted manuscript has been authored by a contractor of the U.S. Government under contract DE-AC05-00OR22725.

NOMENCLATURE

CDD_{65} = cooling degree days with 65°F (18.3°C) base

HDD_{65} = heating degree days with 65°F (18.3°C) base

R_{SI} = thermal resistance in units of $m^2 \cdot K/W$

R_{US} = thermal resistance in units of $h \cdot ft^2 \cdot °F/Btu$

Nu = Nusselt number

Ra = Rayleigh number

REFERENCES

Arnold, J.N., P.N. Bonaparte, I. Canton and D.K. Edwards. 1974. Proceedings of the 1974 Heat Transfer and Fluid Mechanics Institute, Stanford University Press. Stanford, CA 1974.

ASHRAE. 1989. Thermal Resistances of Plane Air Spaces, Chapter 22.2, Table 2. *ASHRAE Handbook—Fundamentals*. Atlanta: ASHRAE.

ASHRAE. 2007. ASHRAE 90.2-2007: *Energy Efficient Design of Low-Rise Residential Buildings*. Atlanta: ASHRAE.

ASTM. American Society for Testing and Materials 2009. Designation C 1549-09: *Standard Test Method for Determination of Solar Reflectance Near Ambient Temperature Using a Portable Solar Reflectometer*. American Society for Testing and Materials, West Conshohocken, PA

ASTM. 2006. *Test Method for Steady-State Heat Flux Measurements and Thermal Transmission Properties by Means of the Heat Flow Meter Apparatus*. Standard C 518. West Conshohocken, Pennsylvania: American Society for Testing and Materials.

ASTM. 2004. Designation C 1371-04a: *Standard Test Method for Determination of Emittance of Materials Near Room Temperature Using Portable Emissometers*. American Society for Testing and Materials, West Conshohocken, PA

ASTM. 2004. ASTM Standard C 1340-04, *Standard Practice for Estimation of Heat Gain or Loss Through Ceilings Under Attics Containing Radiant Barriers by Use of a Computer Program*. West Conshohocken, PA: American Society for Testing and Materials.

Azevedo, L.F. and Sparrow, E.M. 1985. Natural Convection in Open-Ended Inclined Channels, *Journal of Heat Transfer*, 1985. Vol. 107, P. 893–901.

Beal, D. and S. Chandra. 1995. The Measured Summer Performance of Tile Roof Systems and Attic Ventilation Strategies in Hot Humid Climates. In *Thermal Performance of the Exterior Envelopes of Buildings* VI, 753–760. Atlanta: ASHRAE.

Brinkworth, B.J. 2000. A procedure for the routine calculation of laminar free and mixed convection in inclined ducts, *International Journal of Heat and Fluid Flow* 21:456–462.

CEC. California Energy Commission. 2008 *Energy Efficiency Standards for Residential and Nonresidential Buildings*. P400-2008-001-CMF. Sacramento: California Energy Commission.

ElSherbiny, S.M., G.D. Raithby and K.G.T. Hollands, Heat Transfer by Natural Convection across Vertical and Inclined Cavities, *J. Heat Transfer*, Vol. 104, pp. 96–102, 1984.

Fairey, P., M. Swami, D. Beal. 1988. RBS Technology: Task 3 Report. Florida Solar Energy Center. Publication Number: FSEC-CR-211-88.

Hollands, K.G.T., T.E. Unny, G.D. Raithby, and L. Konicek. 1976. Free convection heat transfer across inclined air layers, *Journal of Heat Transfer* May: 189–193.

International Energy Conservation Code (IECC), 2012.

Miller, W. A. 2011. Roof and Attic Design Guidelines for Hot Climates, DOE Deliverable to BTO TM Marc LaFrance.

Miller, W.A. and J., Kosny. 2008. Next Generation Roofs and Attics for Homes, in ACEEE Summer Study on Energy Efficiency in Buildings, proceedings of American Council for an Energy Efficient Economy, Asilomar Conference Center in Pacific Grove, CA., Aug. 2008.

Miller, W. A., M. Keyhani, T. Stovall and A. Youngquist. 2007. Natural Convection Heat Transfer in Roofs with Above-Sheathing Ventilation, in *Thermal Performance of the Exterior Envelopes of Buildings X*. Atlanta: ASHRAE.

Miller, W.A. 2006. The Effects of Infrared-Blocking Pigments and Deck Venting on Stone-Coated Metal Residential Roofs. ORNL/TM-2006/9. Oak Ridge, Tennesse: Oak Ridge National Laboratory.

Miller, W.A., W.M. MacDonald, A.O. Desjarlais, J.A. Atchley, M. Keyhani, R. Olson, and J. Vandewater. 2005. Experimental analysis of the natural convection effects observed within the closed cavity of tile roofs. Presented at Cool Roofs: Cutting Through the Glare, RCI Foundation Conference, Atlanta, May 12–13.

NREL/TP-472-7332a. 1995. Home Energy Rating System Building Energy Simulation Test (HERS BESTEST), Volume 1, used with EnergyPlus: DOE's Next Generation Simulation Program.

Parker, D.S., Sonne, J. K., Sherwin, J. R. 2002. Comparative Evaluation of the Impact of Roofing Systems on Residential Cooling Energy Demand in Florida, in ACEEE Summer Study on Energy Efficiency in Buildings, proceedings of American Council for an Energy Efficient Economy, Asilomar Conference Center in Pacific Grove, CA., Aug. 2002.

Quarles, S.L. and A. TenWolde. 2004. Attic and crawlspace ventilation: Implications for homes located in the Urban-Wildland Interface, Proceedings of the Woodframe Housing Durability and Disaster Issues Conference, Forest Products Society, Las Vegas, October 2004.

Yarbrough, D.W. and Desjarlais, A.O. 1991. Prediction of the Thermal Performance of Single and Multi-Airspace reflective Insulation Materials, *Insulation Materials: Testing and Applications*, 2nd Volume, ASTM STP 1116,Graves and D.C. Wysocki, Eds. American Society for Testing and Materials, Philadelphia.

APPENDIX A

Table A1. Clay and Concrete Tile Specifications for Air Space with Tile Attached Directly to the Roof Deckand also Offset Mounted from the Roof Deck on Battens and Double Batten Assemblies

Manufacturer	Tile Profile	Material	Roof Application	Volume of Air Space for 100 ft^2 of Tile Roof		Average Thickness of Air Space of Tile Roof	
				in.^{3}	m^3	in.	m
MCA Corona Tapered M	High	Clay	Direct-to-Deck	21398	0.351	1.49	0.0378
MCA Classic S	High	Clay	Direct-to-Deck	24746	0.406	1.72	0.0437
MCA Mission S	High	Clay	Direct-to-Deck	25828	0.423	1.79	0.0455
Boral Saxony 900	Flat	Concrete	Direct-to-Deck	16499	0.270	1.15	0.0291
	Flat	Concrete	Battens	20082	0.329	1.39	0.0354
	Flat	Concrete	Double Battens	23771	0.390	1.65	0.0419
Boral Barcelona 900	High	Concrete	Direct-to-Deck	34652	0.568	2.41	0.0611
	High	Concrete	Battens	38670	0.634	2.69	0.0682
	High	Concrete	Double Battens	44047	0.722	3.06	0.0777
Boral Standard Villa	Medium	Concrete	Direct-to-Deck	20088	0.329	1.40	0.0354
	Medium	Concrete	Battens	24195	0.396	1.68	0.0427
	Medium	Concrete	Double Battens	29052	0.476	2.02	0.0512
Boral Espana	High	Concrete	Direct-to-Deck	35948	0.589	2.50	0.0634
	High	Concrete	Battens	36727	0.602	2.55	0.0648
	High	Concrete	Double Battens	42788	0.701	2.97	0.0755
Boral Madera	Flat	Concrete	Direct-to-Deck	7833	0.128	0.54	0.0138
	Flat	Concrete	Battens	17133	0.281	1.19	0.0302
	Flat	Concrete	Double Battens	22440	0.368	1.56	0.0396
Eagle	Flat	Concrete	Direct-to-Deck	16313	0.267	1.13	0.0288
	Flat	Concrete	Battens	26342	0.432	1.83	0.0465
	Flat	Concrete	Double Battens	31427	0.515	2.18	0.0554

APPENDIX B

The Barcelona 900™ is an extruded interlocking concrete roof tile that complies with ASTM C 1492. The tile is a popular selection among homeowners because it reflects the classic style of historic Spanish architecture. It has distinct hue combinations that create an aesthetically pleasing and rustic look. The tile is made of concrete. About 85 tiles are needed for coverage of 100 square feet (9.3 m^2) of roof coverage. Tile weight is reported at 900 lb (431 kg) for 100 square feet (9.3 m^2) of coverage. Tables B1, B2, and B3 list the equivalent annual thermal resistance of the tile for direct-to-deck, batten and double batten applications simulated for the 8 ASHRAE climatic zones (Table 2) and also for Sacramento, CA assuming Title 24 code requirements.

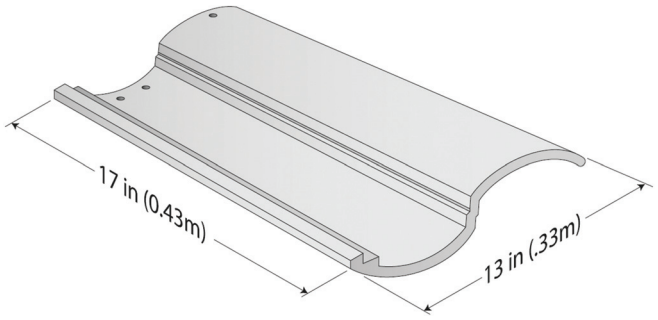

Figure B1 *Barcelona 900 Concrete Tile.*

Table B1. Barcelona 900 Effective Annual Thermal Resistance [R_{US}] of Inclined Air Space Yielding Same Ceiling Load as Direct-to-Deck Asphalt Shingle Roof. Air Space Effective Emittance = 0.82

Roof Configuration	Air Space Height, in. (mm)	ASHRAE Climate Zones								Sacramento, CA
		1	2	3	4	5	6	7	8	Title 24
Direct-to-Deck	2.406 (61.1)	2.72	1.42	0.68	0.29	0.08	0.05	0.00	0.17	0.52
Battens	2.69 (68.2)	2.84	1.47	0.71	0.30	0.09	0.05	0.00	0.16	0.55
Double Battens	3.058 (77.7)	2.97	1.54	0.74	0.32	0.09	0.05	–0.01	0.16	0.58

R_{US} units = [(h · ft^2 · °F)/Btu]; R_{SI} [(m^2 · K)/W] = R_{US} ÷ 5.678263
A solar reflectance of 0.10 and thermal emittance of 0.90 was assumed for control shingle and for Barcelona 900 simulations.

Table B2. Barcelona 900 Effective Annual Thermal Resistance [R_{US}] of Inclined Air Space Yielding Same Ceiling Load as Direct-to-Deck Asphalt Shingle Roof. Air Space Effective Emittance = 0.22

Roof Configuration	Air Space Height, in. (mm)	ASHRAE Climate Zones								Sacramento, CA
		1	2	3	4	5	6	7	8	Title 24
Direct-to-Deck	2.406 (61.1)	5.66	3.20	1.86	0.99	0.51	0.36	0.23	0.35	2.10
Battens	2.69 (68.2)	5.83	3.29	1.91	1.01	0.52	0.36	0.23	0.35	2.15
Double Battens	3.058 (77.7)	6.03	3.38	1.95	1.03	0.53	0.36	0.23	0.34	2.21

R_{US} units = [(h · ft^2 · °F) / Btu]; R_{SI} [(m^2 · K)/W] = R_{US} ÷ 5.678263
A solar reflectance of 0.10 and thermal emittance of 0.90 was assumed for control shingle and for Barcelona 900 simulations.

Table B3. Barcelona 900 Effective Annual Thermal Resistance [R_{US}] of Inclined Air Space Yielding Same Ceiling Load as Direct-to-Deck Asphalt Shingle Roof. Air Space Effective Emittance = 0.05

Roof Configuration	Air Space Height, in. (mm)	ASHRAE Climate Zones								Sacramento, CA
		1	2	3	4	5	6	7	8	Title 24
Direct-to-Deck	2.406 (61.1)	8.54	4.79	2.81	1.50	0.80	0.56	0.37	0.42	3.29
Battens	2.69 (68.2)	8.75	4.89	2.87	1.53	0.81	0.57	0.37	0.42	3.35
Double Battens	3.058 (77.7)	9.02	5.02	2.93	1.56	0.82	0.57	0.37	0.42	3.42

R_{US} units = [(h · ft^2 · °F) / Btu]; R_{SI} [(m^2 · K)/W] = R_{US} ÷ 5.678263
A solar reflectance of 0.10 and thermal emittance of 0.90 was assumed for control shingle and for Barcelona 900 simulations.

The Villa 900 concrete tile has a moderate tile profile whose shape and style of tile is often seen on buildings in Italy and Southern France. About 85 tiles will cover 100 square feet (9.3 m^2) of roof. Tile weight is about 920 lbs (417.2 kg) per 100 square feet (9.3 m^2) of coverage. Tables B4, B5 and B6 list the equivalent annual thermal resistance of the tile for direct-to-deck, batten and double batten applications simulated for the eight ASHRAE climatic zones (Table 2) and also for Sacramento, California assuming Title 24 code requirements.

The MCA Corona and Classic S Tapered M tiles are a two-piece pan and cover units. The clay tiles are extruded and fire cured and comply with ASTM C 1167. The tile meets all freeze/thaw and intrusive salt environments. About 150 tiles are needed for 100 square feet (9.3 m^2) of roof coverage. Tile weight is reported at 1050 lb (476.2 kg)

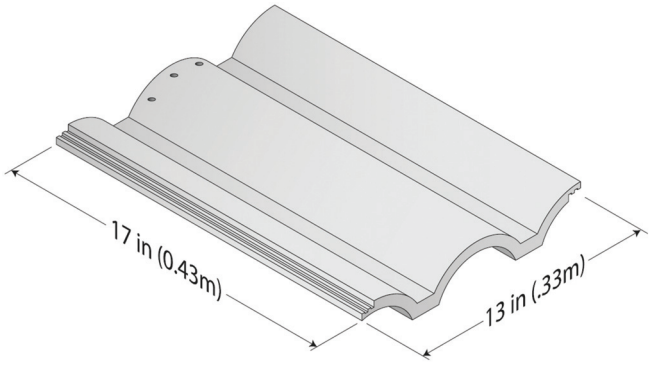

Figure B2 *Villa 900 Concrete Tile.*

Table B4. Villa 900 Effective Annual Thermal Resistance [R_{US}] of Inclined Air Space Yielding Same Ceiling Load as Direct-to-Deck Asphalt Shingle Roof. Air Space Effective Emittance = 0.82

Roof Configuration	Air Space Height, in. (mm)	ASHRAE Climate Zones								Sacramento, CA
		1	2	3	4	5	6	7	8	Title 24
Direct-to-Deck	1.4 (35.6)	2.21	1.14	0.53	0.23	0.06	0.05	0.00	0.17	0.37
Battens	1.68 (42.7)	2.37	1.23	0.58	0.25	0.07	0.05	0.00	0.17	0.42
Double Battens	2.02 (51.3)	2.55	1.32	0.63	0.27	0.08	0.05	0.00	0.17	0.47

R_{US} units = [(h · ft^2 · °F) / Btu]; R_{SI} [(m^2 · K)/W] = R_{US} ÷ 5.678263
A solar reflectance of 0.10 and thermal emittance of 0.90 was assumed for control shingle and for Villa 900 simulations.

Table B5. Villa 900 Effective Annual Thermal Resistance [R_{US}] of Inclined Air Space Yielding Same Ceiling Load as Direct-to-Deck Asphalt Shingle Roof. Air Space Effective Emittance = 0.22

Roof Configuration	Air Space Height, in. (mm)	ASHRAE Climate Zones								Sacramento, CA
		1	2	3	4	5	6	7	8	Title 24
Direct-to-Deck	1.4 (35.6)	4.91	2.81	1.66	0.89	0.47	0.34	0.22	0.34	1.87
Battens	1.68 (42.7)	5.15	2.94	1.72	0.92	0.49	0.34	0.22	0.35	1.94
Double Battens	2.02 (51.3)	5.40	3.07	1.79	0.95	0.50	0.35	0.22	0.35	2.02

R_{US} units = [(h · ft^2 · °F) / Btu]; R_{SI} [(m^2 · K)/W] = R_{US} ÷ 5.678263
A solar reflectance of 0.10 and thermal emittance of 0.90 was assumed for control shingle and for Villa 900 simulations.

Table B6. Villa 900 Effective Annual Thermal Resistance [R_{US}] of Inclined Air Space Yielding Same Ceiling Load as Direct-to-Deck Asphalt Shingle Roof. Air Space Effective Emittance = 0.05

Roof Configuration	Air Space Height, in. (mm)	ASHRAE Climate Zones								Sacramento, CA
		1	2	3	4	5	6	7	8	Title 24
Direct-to-Deck	1.4 (35.6)	7.61	4.32	2.55	1.37	0.75	0.52	0.35	0.40	2.99
Battens	1.68 (42.7)	7.90	4.46	2.63	1.41	0.77	0.54	0.36	0.41	3.08
Double Battens	2.02 (51.3)	8.21	4.62	2.72	1.45	0.79	0.55	0.36	0.42	3.18

R_{US} units = [(h · ft^2 · °F) / Btu]; R_{SI} [(m^2 · K)/W] = R_{US} ÷ 5.678263
A solar reflectance of 0.10 and thermal emittance of 0.90 was assumed for control shingle and for Villa 900 simulations.

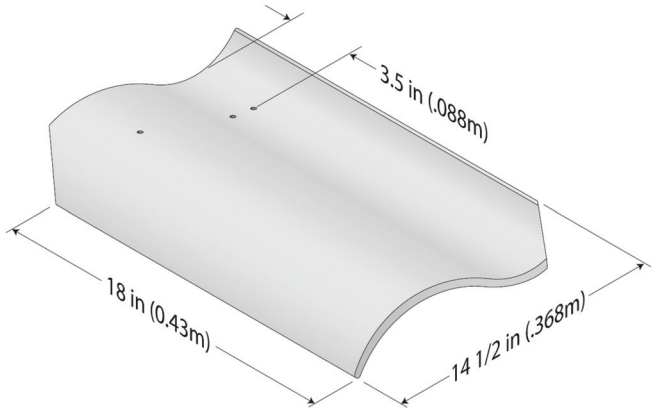

Figure B3 *MCA Corona tapered M clay tile.*

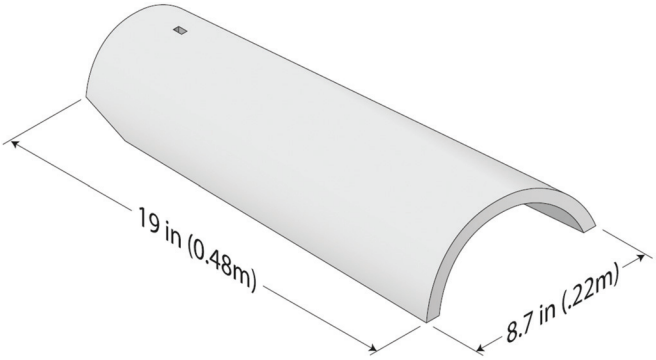

Figure B4 *MCA Classic S tapered M clay tile.*

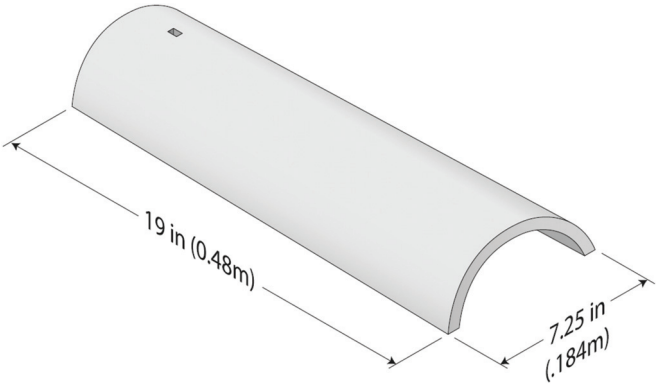

Figure B5 *MCA Mission S clay tile.*

for 100 square feet (9.3 m^2) of coverage. The Mission S style is a one-piece tile with weight of 780 lb (353.7 kg) for 100 square feet (9.3 m^2) of coverage. Tables B7, B8, and B9 list the equivalent annual thermal resistance of the tile for direct-to-deck applications simulated for the eight ASHRAE climatic zones (Table 2) and also for Sacramento, California, assuming Title 24 code requirements.

Table B7. MCA Effective Annual Thermal Resistance [R_{US}] of Inclined Air Space Yielding Same Ceiling Load as Direct-to-Deck Asphalt Shingle Roof. Air Space Effective Emittance = 0.82

Roof Configuration	Air Space Height, in. (mm)	ASHRAE Climate Zones								Sacramento, CA
		1	2	3	4	5	6	7	8	Title 24
Corona Tapered M	1.49 (37.8)	2.23	1.13	0.50	0.21	0.04	0.03	–0.01	0.17	0.29
Classic S Tapered M	2.24 (56.8)	2.36	1.20	0.54	0.23	0.05	0.04	–0.01	0.17	0.33
Mission S	2.99 (75.9)	2.40	1.22	0.55	0.23	0.05	0.04	–0.01	0.17	0.34

R_{US} units = [(h · ft^2 · °F) / Btu]; R_{SI} [(m^2 · K)/W] = R_{US} ÷ 5.678263
MCA clay tile fastened directly to the roof deck without batten system.
A solar reflectance of 0.10 and thermal emittance of 0.90 was assumed for control shingle and for Corona Tapered clay tile simulations.

Table B8. MCA Effective Annual Thermal Resistance [R_{US}] of Inclined Air Space Yielding Same Ceiling Load as Direct-to-Deck Asphalt Shingle Roof. Air Space Effective Emittance = 0.22

Roof Configuration	Air Space Height, in. (mm)	ASHRAE Climate Zones								Sacramento, CA
		1	2	3	4	5	6	7	8	Title 24
Corona Tapered M	1.49 (37.8)	4.95	2.82	1.64	0.87	0.46	0.33	0.21	0.34	1.81
Classic S Tapered M	2.24 (56.8)	4.95	2.82	1.64	0.87	0.46	0.33	0.21	0.34	1.81
Mission S	2.99 (75.9)	4.95	2.82	1.64	0.87	0.46	0.33	0.21	0.34	1.81

R_{US} units = [(h · ft^2 · °F) / Btu]; R_{SI} [(m^2 · K)/W] = R_{US} ÷ 5.678263
MCA clay tile fastened directly to the roof deck without batten system.
A solar reflectance of 0.10 and thermal emittance of 0.90 was assumed for control shingle and for Corona Tapered clay tile simulations.

Table B9. MCA Clay Tile Effective Annual Thermal Resistance [R_{US}] of Inclined Air Space Yielding Same Ceiling Load as Direct-to-Deck Asphalt Shingle Roof. Air Space Effective Emittance = 0.05

Roof Configuration	Air Space Height, in. (mm)	ASHRAE Climate Zones								Sacramento, CA
		1	2	3	4	5	6	7	8	Title 24
Corona Tapered M	1.49 (37.8)	7.67	4.33	2.54	1.36	0.74	0.52	0.34	0.40	2.95
Classic S Tapered M	2.24 (56.8)	7.90	4.45	2.61	1.39	0.76	0.53	0.35	0.41	3.03
Mission S	2.99 (75.9)	7.96	4.48	2.63	1.40	0.76	0.53	0.35	0.41	3.05

R_{US} units = [(h · ft^2 · °F) / Btu]; R_{SI} [(m^2 · K)/W] = R_{US} ÷ 5.678263
MCA clay tile fastened directly to the roof deck without batten system.
A solar reflectance of 0.10 and thermal emittance of 0.90 was assumed for control shingle and for MCA clay tile simulations.